Epilepsy Research (2012) 99, 78—86

journal homepage: www.elsevier.com/locate/epilepsyres

Localization of ictal onset zones in Lennox—Gastaut syndrome (LGS) based on information theoretical time delay analysis of intracranial electroencephalography (iEEG)

Jae-Hyun Cho[a,c,1], Hoon-Chul Kang[b,1], Young-Jin Jung[a,f], Yong-Ho Lee[d], Ki-Young Jung[e], Heung Dong Kim[b], Chang-Hwan Im[a,*]

[a] Department of Biomedical Engineering, Hanyang University, Seoul, South Korea
[b] Department of Pediatrics, Yonsei University College of Medicine, Seoul, South Korea
[c] Department of Biomedical Engineering, Yonsei University, Wonju, South Korea
[d] Korea Institute of Standard and Sciences (KRISS), Daejeon, South Korea
[e] Department of Neurology, Korea University College of Medicine, Seoul, South Korea
[f] Research Institute of Industrial Science, Hanyang University, Seoul, South Korea

Received 28 July 2011; received in revised form 9 October 2011; accepted 15 October 2011
Available online 8 November 2011

KEYWORDS
Ictal onset zones;
Intracranial electroencephalography (iEEG);
Lennox—Gastaut syndrome (LGS);
Mutual information;
Secondary generalized epilepsy;
Time delay estimation

Summary Precise localization of ictal onset zones is of great clinical importance for successful surgery in patients with intractable drug-resistant epilepsy. Time delay analysis has been one of the most reliable and most widely used computational electroencephalogram (EEG) analysis methods for localizing ictal onset zones. However, the majority of previous studies have only been applied to the localization of ictal onset zones in focal epilepsy. In the present study, we analyzed intracranial EEG (iEEG) recordings acquired from patients with Lennox—Gaustaut syndrome (LGS), which is a type of intractable, pediatric, secondary generalized epilepsies with bilaterally synchronous ictal epileptiform discharges. To estimate the ictal onset zones from ictal iEEG recordings, we estimated time delays among iEEG signals based on the information theoretical approach. The results of the time delay analysis applied to the iEEG data of four successfully treated LGS patients corresponded well with the surgical resection areas identified by experienced epileptologists and multiple neuroimaging modalities, suggesting that the time delay analysis may provide useful information on the precise locations of ictal onset zones prior to epilepsy surgery in LGS patients.

* Corresponding author at: Department of Biomedical Engineering, Hanyang University, 17 Haengdang-dong, Seongdong-gu, Seoul 133-791, South Korea. Tel.: +82 2 2220 2322; fax: +82 2 2296 5943.
E-mail address: ich@hanyang.ac.kr (C.-H. Im).
[1] These two authors contributed equally to this work.

0920-1211/$ — see front matter © 2011 Elsevier B.V. All rights reserved.
doi:10.1016/j.eplepsyres.2011.10.024

Introduction

Precise localization of epileptogenic zones is one of the most important factors for the successful surgical treatment of patients with intractable drug-resistant epilepsies. Among the various neuroimaging modalities for localizing the seizure generators, such as electroencephalography (EEG), magnetoencephalography (MEG), positron emission tomography (PET), and single photon emission computed tomography (SPECT), intracranial electroencephalography (iEEG) has been regarded as the most reliable modality because it can record both ictal and interictal epileptiform brain activities directly from a cortical surface with minimal signal distortions (Binnie et al., 1994; Behrens et al., 1994; Dubeau and McLachlan, 2000; Rosenow and Lüders, 2001; Pondal-Sordo et al., 2007). Traditionally, localization of ictal onset zones was performed by epileptologists through visual inspection of iEEG recordings. For example, ictal onset zones are usually found in locations with sustained rhythmic changes on electrocorticogram (ECoG) accompanied by subsequent clinically typical seizure activity. In many practical cases, however, it is difficult even for very experienced epileptologists to distinguish ictal onset zones from irritative zones activated by propagation through visual inspection of ictal epileptiform activities, and thus the determination of ictal onset zones was sometimes highly dependent upon the epileptologists who participated in the pre-surgical evaluation process (Wilson and Emerson, 2002).

Recently, in order to confirm the visual inspection results and further assist the final decision of areas for surgical resection, various computational EEG analysis methods have been introduced and used to identify ictal onset zones of intractable epilepsies. To identify the ictal onset zones, various functional connectivity measures have been adopted, such as mutual information (Mars and Lopes da Silva, 1987) and directed transfer functions (DTFs) (Ding et al., 2007; Swiderski et al., 2009; Wilke et al., 2010). Despite extensive studies on computational EEG analysis methods, most studies have focused only on the localization of ictal onset zones in focal epilepsy; whereas only a few studies have reported the possibility of computational EEG analyses for the localization of ictal onset zones in secondary generalized epilepsy (Jung et al., 2011). In the case of secondary generalized epilepsy, identification of ictal onset zones is generally more difficult and complicated than that in focal epilepsy due to its generalized ictal epileptiform discharges. Therefore, one of the challenging issues in epilepsy research is the precise localization of ictal onset zones in secondary generalized epilepsy.

Of the various computational EEG analysis methods, time delay estimation has been widely used to localize epileptic foci in ictal/interictal iEEG and to identify network characteristics of epileptic seizure activities (Brazier, 1972; Gotman, 1981, 1983; Mars and Lopes Da Silva, 1983; Mars et al., 1985; Kobayashi et al., 1992; Medvedev et al., 1996; Meeren et al., 2002) because this method has the potential to accurately identify temporally leading channels even when the recorded EEG signals possess very small time differences. However, most of the previous studies focused only on focal epilepsy, and only a few studies have applied the time delay analysis to generalized epilepsy. Medvedev et al. (1996) and Meeren et al. (2002) applied time delay analysis to epileptic animal models with primary generalized epilepsy and revealed the existence of cortical foci that derived epileptic networks. Gotman (1983) and Mars et al. (1985) independently applied time delay estimation to the delineation of epileptogenesis in human patients with generalized epilepsy but did not apply the approach to the localization of ictal onset zones. Despite these extensive studies, however, time delay analysis has not been applied to the localization of ictal onset zones in human secondary generalized epilepsy.

In the present study, Lennox—Gastaut syndrome (LGS) was selected as the target epilepsy type since localization of ictal onset zones in LGS is critical for surgical treatment, as in focal epilepsy. Some patients with LGS have focal lesions that attribute to secondary generalized epileptic encephalopathy; these focal lesions are generally identified via EEG, MRI, and other functional neuroimaging techniques (Wyllie et al., 2007; Lee et al., 2010a). Recently, several groups, including ours, have reported successful outcomes after resective epilepsy surgery in children with LGS. However, identification of the focal lesions was possible only in limited cases, and the conventional imaging modalities only provided broad spatial information on the potential epileptogenic zones (Kim et al., 2009; Lee et al., 2010a). Therefore, additional quantitative techniques to confirm the locations of ictal onset zones are still required.

The aim of this study was to localize ictal onset zones in LGS patients by estimating time delays between iEEG signals at seizure onset and to visualize the potential epileptogenic zones on individual anatomical structures. We then compared the results of time delay analysis with those of conventional DTF analysis as well as surgical resection areas in order to investigate the feasibility of using time delay analysis in the pre-surgical evaluation of patients with LGS.

Methods

Patients

Among 27 pediatric patients who had LGS and underwent resective epilepsy surgery during 2001—2007 in Severance Children's Hospital of Korea, 16 patients have been seizure-free since surgery. In these seizure-free cases, four patients without cerebral infarctions or progressive underlying metabolic diseases or chromosomal anomalies were included in the present study (Table 1). We used the following three screening criteria to select the analysis datasets: (1) in these patients, up to 30% of preoperative epileptiform discharges were generalized and/or generalized contralateral maximum or multiregional epileptiform discharges; (2) they had normal or nearly normal brain MRI findings without definite brain lesions including cerebral infarctions or progressive cortical atrophy or malformation of cortical development and so on. In these patients, neuroimaging was not so helpful to localize the epileptogenic area; (3) after the surgery, they were maintaining complete seizure free state without any suspicious seizure attacks till then. Patients who did not satisfy all the above criteria were excluded from our study and our analysis were applied only to the selected patients' iEEG datasets. Parents or guardians of all four LGS patients provided written consent, which was approved by the Institutional Review Boards of Severance Hospital, before their child's data were enrolled in this study. Table 1 summarizes the demographic data and the characteristics of the enrolled patients.

Table 1 Patient demographics and characteristics.

Patient	1 (LYS)	2 (JMS)	3 (SWJ)	4 (KOG)
Age at surgery	3	2	3	17
Sex	Male	Male	Male	Male
Age at first epilepsy development	7 months	5 months	18 months	12 years
Semiology	Generalized tonic spasms and head drops	Head drops and atypical absences	Generalized tonic spasms and staring spells	Generalized tonic seizures of both arms
MRI	Normal	Blurring of the gray-white matter interface on right frontal lobe	Suspicious but not definite cortical thickening on right frontal lobe	Blurring of the gray-white matter interface on right frontal lobe
FDG-PET	Normal	Normal	Focal hypometabolism on right frontal lobe	Hypometabolism on right frontal lobe
Ictal SPECT	Lateralized consistently to right frontotemporal area	Unsuccessful	Lateralized consistently to right frontotemporal area	Unsuccessful
Video-EEG	Right frontotemporal area (refer to the text)	Right frontal area (refer to the text)	Right frontotemporal area (refer to the text)	Right frontal area (refer to the text)
Surgery	(Twice) (1) right frontal lobe → (2) posterior margin of the pre-resection site	(Once) Right frontal lobe & right anterior temporal lobe	(Twice) (1) right frontal lobe → (2) right inferior frontal gyrus & right temporal lobe	(Once) Right frontal lobe
Outcome	Seizure free	Seizure free	Seizure free	Seizure free
Pathologic result	Focal cortical dysplasia	Focal cortical dysplasia	Focal cortical dysplasia	Focal cortical dysplasia
EEG after operation	Nearly normalized background activities and no epileptiform discharge	Nearly normalized background activities only with occasional multifocal sharp waves	Nearly normalized background activities and no epileptiform discharge	Nearly normalized background activities and no epileptiform discharge
No. subdural electrodes	104	100	116	120
No. ictal events in iEEG recordings	20	16	19	19

The first subject (LYS) was a three-year-old boy with severe mental impairment (Intelligence Quotient (IQ) of 25) who had suffered from refractory epilepsy since seven months of age. Two types of seizures were observed in this subject, generalized tonic spasms and head drops, and none of the available antiepileptic medications could suppress his seizures. Continuous video EEG monitoring showed frequent generalized slow spikes and waves and generalized paroxysmal fast activities, as well as localized epileptiform discharges or bisynchronous sharp waves predominantly located in the right frontotemporal areas. Ictal EEG showed generalized slow waves followed by low-voltage fast activity during generalized tonic seizures or head drops but did not aid in the lateralization of the epileptogenic area. Based on the results of a Phase I study and ictal/interictal iEEG monitoring, the patient underwent a right frontal resection at 3 years of age and was free of seizures for 2.5 years before his seizures recurred at 6 years of age. The posterior margin of the pre-resection site was further resected, and the patient has been free of seizures for 1.6 years (see Fig. 3 for the final resection areas marked on the electrode grids).

The second subject (JMS) was a 2-year-old boy with severe mental impairment, who had suffered from refractory epilepsy since 5 months of age. Seizures presented as head drops and were intractable to several available antiepileptic medications. Continuous video EEG monitoring consistently showed abundant generalized slow spikes and waves and generalized paroxysmal fast activities, as well as localized epileptiform discharges in the right frontal area. Ictal EEG showed generalized slow waves followed by electrodecremental fast activities during head drops, but did not aid in the lateralization of the epileptogenic area. According to the results of a Phase I study and ictal/interictal iEEG monitoring, the right frontal area and right anterior temporal lobe (see Fig. 3 for the resection area) were resected during surgery. This patient has been free of seizures for 5.6 years without medication.

The third subject (SWJ) was a 3-year-old boy with severe mental impairment (IQ of 29) who had developed refractory epilepsy at 18 months of age. This patient presented with two types of seizures, generalized tonic spasms and staring spells, which were not suppressed with available antiepileptic medications. Continuous video EEG monitoring showed frequent generalized slow spikes and waves, generalized paroxysmal fast activities, and localized epileptiform discharges or bisynchronous sharp waves in the right frontotemporal areas. Ictal EEG showed generalized slow waves followed by low-voltage fast activities during generalized tonic seizures, but did not aid in the lateralization of the epileptogenic area. Based on the results of a Phase I study and ictal/interictal iEEG monitoring, the patient underwent a right frontal resection when he was 3 years old, which reduced the frequency of his seizures but did not control them completely. The right inferior frontal gyrus and right temporal area were further resected, and this subject has been free of seizures for 1.6 years on a reduced number of medications (see Fig. 3 for the final resection areas).

The fourth subject (KOG) was a 16-year-old boy with moderate mental impairment (IQ of 45) who had suffered from refractory epilepsy since 12 years of age. Seizures presented as generalized tonic seizures of both arms for 10—15 s, 5—6 times per day. No available antiepileptic medication suppressed his seizures. Baseline interictal awake EEG showed contralateral localized epileptiform discharges and exclusively generalized epileptiform discharges, such as generalized slow spikes and waves and generalized paroxysmal fast activities. During the interictal burst, there was no change in his behavior. Ictal EEG shows generalized slow waves followed by low-voltage fast activities during generalized tonic seizure, but did not aid in the lateralization of the epileptogenic area. The patient underwent a right frontal lobectomy (see Fig. 3 for the resection area) at 17 years of age and has been free of seizures for 2.5 years without medication.

Determination of areas for surgical resection

As described in the previous section, we used a variety of neuroimaging modalities to determine surgical resection areas. All subjects were examined using a video-EEG monitoring system with electrodes placed according to the international 10—20 system to define the semiology of habitual seizures and to identify epileptogenic foci. Epileptogenic areas were delineated primarily through interpretation of EEG data, and other imaging modalities, such as MRI, PET, and SPECT, were used to reinforce these findings. iEEG monitoring using subdural electrodes was also used to determine margins for surgical resection. Preoperative and intraoperative functional mapping and intraoperative ECoG were also performed when necessary (Kim et al., 2009; Lee et al., 2010b).

The surgical area was defined based on the clinical, neuroimaging, and electrophysiological results. The resection margin for epilepsy of a neocortical origin was defined by: (1) the presence of either a discrete lesion on MRI and functional neuroimages compatible with ictal or interictal iEEG, (2) various interictal intracranial EEG findings, including >3 repetitive spikes per second, runs of repetitive spike and slow wave discharges, localized or spindle-shaped fast activities and electrodecremental fast activities, and (3) the absence of an eloquent cortex. The diagnosis and classification of pathologic cortical dysplasia (CD) were made according to the system of Palmini et al. (2004).

iEEG data acquisition

The ictal iEEG recordings were obtained from a multichannel digital EEG acquisition system (Telefactor, Grass Technologies) at a sampling rate of 200 Hz. The locations of the silastic subdural grid and strip electrodes were determined based on multiple neuroimaging data (see Fig. 3 for the grid and strip electrode positions). The recorded iEEG data were reviewed by an epileptologist, and 16—20 seizures were observed in each subject (see Table 1). Seizure onset times were identified visually by the epileptologist with the aid of video monitoring. Fig. 1 shows an example of the ictal iEEG signals recorded by 104 electrodes from subject 1 (LYS); these signals are segmented with respect to the ictal onset time centered at 5 s. No specific pre-processing procedures except for baseline correction and 60 Hz notch filtering were applied to the raw iEEG data.

Time delay estimation based on mutual information

In the present study, ictal iEEG recordings acquired from four LGS patients were analyzed using the time delay estimation based on mutual information (Moddemeijer, 1988; Talantzis et al., 2005), in order to localize ictal onset zones.

Assuming two discrete time signals, x_n and y_n, acquired from different electrode locations, we define a part of length M of signal x_n with a start index m (denoted as $F_x(m; M)$) and a part of length

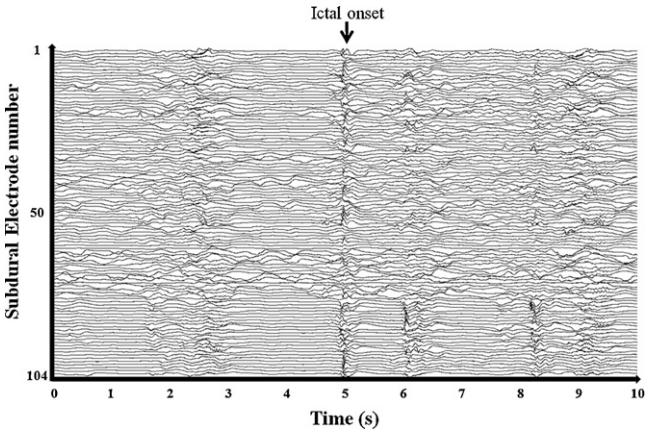

Figure 1 An example of ictal iEEG signals from subject 1 (LYS) recorded using 104 electrodes. The signal was segmented with respect to the ictal onset time, centered at 5 s. No specific pre-processing procedures except for baseline correction and 60 Hz notch filtering were applied to the raw iEEG data.

M of the other signal y_n with a shifted start index $m+j$ (denoted as $F_y(m+j; M)$), as follows:

$$\begin{aligned} F_x(m; M) &= (x_m, x_{m+1}, \ldots, x_{m+M-1})^T \\ F_y(m+j; M) &= (y_{m+j}, y_{m+j+1}, \ldots, y_{m+j+M-1})^T \end{aligned} \tag{1}$$

where the superscript 'T' represents the transpose. Then, the mutual information between two signals $F_x(m; M)$ and $F_y(m+j; M)$ can be defined as

$$I\left\{F_x(m; M), F_y(m+j; M)\right\} = -\frac{1}{2}\log\frac{\det C(j)}{\det C_{xx}\det C_{yy}}, \tag{2}$$

where $m = 1,\ldots,N_m$ (the number of time samples), det() is the determinant operator, and $C(j)$ is the covariance matrix of the signals, which is defined as

$$C(j) = E\left\{\begin{bmatrix} F_x(m; M) \\ F_y(m+j; M)\end{bmatrix}\cdot\begin{bmatrix} F_x(m; M) \\ F_y(m+j; M)\end{bmatrix}^T\right\} = \begin{bmatrix} C_{xx} & C_{xy}(j) \\ C_{yx}(j) & C_{yy}\end{bmatrix}, \tag{3}$$

where E is the expected value operator, C_{xx} is the auto-covariance matrix of x, C_{yy} is the auto-covariance matrix of y, $C_{xy}(j)$ is the cross-covariance matrix of x and j-shifted y, and $C_{yx}(j)$ is the cross-covariance matrix of y and j-shifted x (Cover et al., 1991).

Then the time delay of y with respect to x, denoted as τ_{xy}, can be defined as the shifted time sample j when the averaged mutual information,

$$I_{\text{avg}}(j) = \frac{1}{N_m}\sum_{m=1}^{N_m} I\left\{F_x(m; M), F_y(m+j; M)\right\}, \tag{4}$$

reaches the maximum value. In the present study, the time delay values between every possible pair of electrodes were calculated for each epoch, consisting of 780 time samples ($N_m = 780$) centered at each ictal onset time. We varied the shifted time sample j from −10 to 10. According to Moddemeijer's report (1988), the proper size of M is required to robustly obtain a single extremum of mutual information, but an M that is too large may lead to excessive computational burden. In our study, $M = 3$ was chosen empirically and fixed during the entire analysis. For the verification of our selection, we varied the M value from 1 to 5, but the different M values did not influence the final distribution patterns.

To determine whether the estimated time delay values were meaningful, we employed statistical significance testing with a

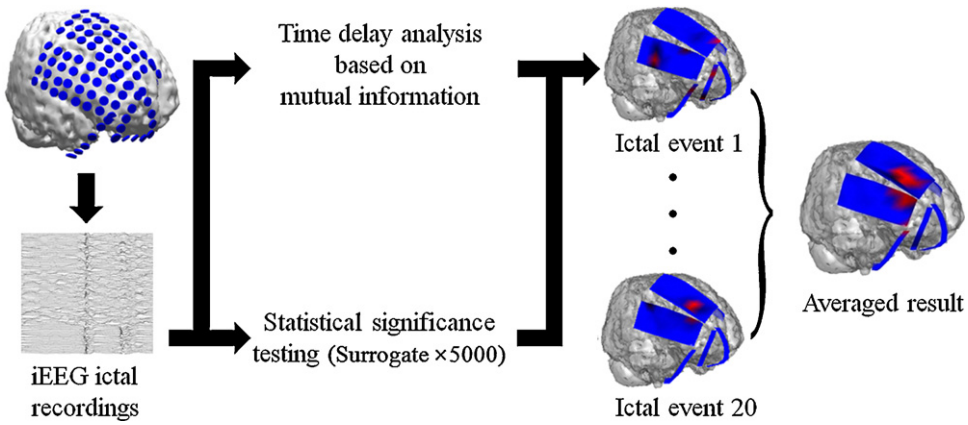

Figure 2 A schematic illustration of the procedures of the present time delay analysis. The time delay analysis method was applied to estimate small time differences between iEEG channels. To determine whether the estimated time delay values were meaningful, we employed a surrogate test and discarded the time delay values from pairs of time series between which any statistically significant relationship could not be found. The average time delay values evaluated for each ictal event were averaged over all ictal events, and the final results were normalized with respect to the maximum absolute value.

surrogate test and discarded the time delay values evaluated from a pair of time series between which any statistically significant relationship (mutual information) could not be found. The surrogate test has been widely used to determine the significance of interactions between brain signals (Theiler et al., 1992). Generally, the temporal correlation between two time signals is destroyed when the phases of two signals are randomly shuffled (Theiler et al., 1992; Schreiber and Schmitz, 1996). In the present study, we generated large surrogate datasets consisting of 5000 data for each pair of electrodes by randomly and independently rearranging the phases of time series (Schreiber, 2000). Then, the empirical distributions of the maximum mutual information values of surrogate data were estimated to determine the significance level, for which we selected the top 1% of values from each distribution ($p = 0.01$). The time delay value between a pair of time series whose maximum mutual information value did not exceed the threshold level was not used in the next analysis steps.

To quantify the time delay value of each electrode, the average time delay of the i-th signal T_i was evaluated as

$$T_i = \frac{1}{k-1} \sum_{\substack{j=1 \\ j \neq i}}^{k} \tau_{ji}, \tag{5}$$

where k is the number of signals having significant maximum mutual information value with the i-th signal, and τ_{ji} is the time delay value between the j-th and i-th electrodes. The average time delay values evaluated for each ictal event were averaged over all ictal events, and the final results were normalized with respect to the maximum absolute value of T_i. All of the above processes were performed using in-house software coded with Matlab 2009a (Mathworks, Inc., USA).

After evaluating the time delay value for each iEEG signal, the distribution of the average time delay values was illustrated on 3D brain images (see Fig. 3). The cortical surface models of the LGS patients were generated from the individual T1-weighted MR images using CURRY6 for Windows (Compumedics, Inc., USA). The locations of the subdural electrodes were obtained from individual CT images and were semi-automatically registered on the segmented cortical surface model using the same software. The resulting distribution maps were generated using Matlab. In the distribution maps, electrodes with higher average time delay values were regarded as probable ictal onset zones. A schematic illustration of these procedures is shown in Fig. 2.

Directed transfer function (DTF)

For the comparison with the time delay estimation results, the DTF method was also implemented. The DTF method has been used for the analysis of causal interactions among several signals over a frequency range of interest (Kaminski and Blinowska, 1991; Eichler, 2006) and was successfully applied to the localization of ictal onset zones in LGS in our previous study (Jung et al., 2011). In this study, the same strategies were applied to the present analysis as were used in our previous study except that the final outflow values were averaged over all ictal events and normalized to the maximum outflow value in each LGS patient. This section describes a very brief introduction of the DTF-based localization of ictal onset zones; more detailed descriptions can be found in our previous work (Jung et al., 2011). The averaged outflow of an i-th was defined as

$$\mathrm{OF}_i = \frac{1}{k-1} \sum_{\substack{j=1 \\ j \neq i}}^{k} \sigma_{ji}, \tag{6}$$

where k is the number of signals, σ_{ji} is the DTF value representing the outflow from signal j to signal i, averaged over the frequency of interest (8—50 Hz in this study). The DTF values were evaluated based on frequency-domain multivariate autoregressive (MVAR) modeling (Strand, 1977; Marple and Nuttall, 1983; Neumaier and Schneider, 2001; Schlögl, 2006) when the model order was determined using the Bayesian information criterion (BIC) (Schwarz, 1978). As in the time delay estimation, the average outflow values were visualized on 3D brain images, and the electrodes with higher average outflow values were regarded as probable ictal onset zones.

Results

We estimated the averaged time delay values and the averaged outflow values of the iEEG signals recorded from four LGS patients and then overlaid the values on the 3D anatomical images of each subject. Fig. 3 shows the surgical resection areas (Fig. 3a, first row), the outflow distributions estimated from the DTF analysis (Fig. 3b, second row),

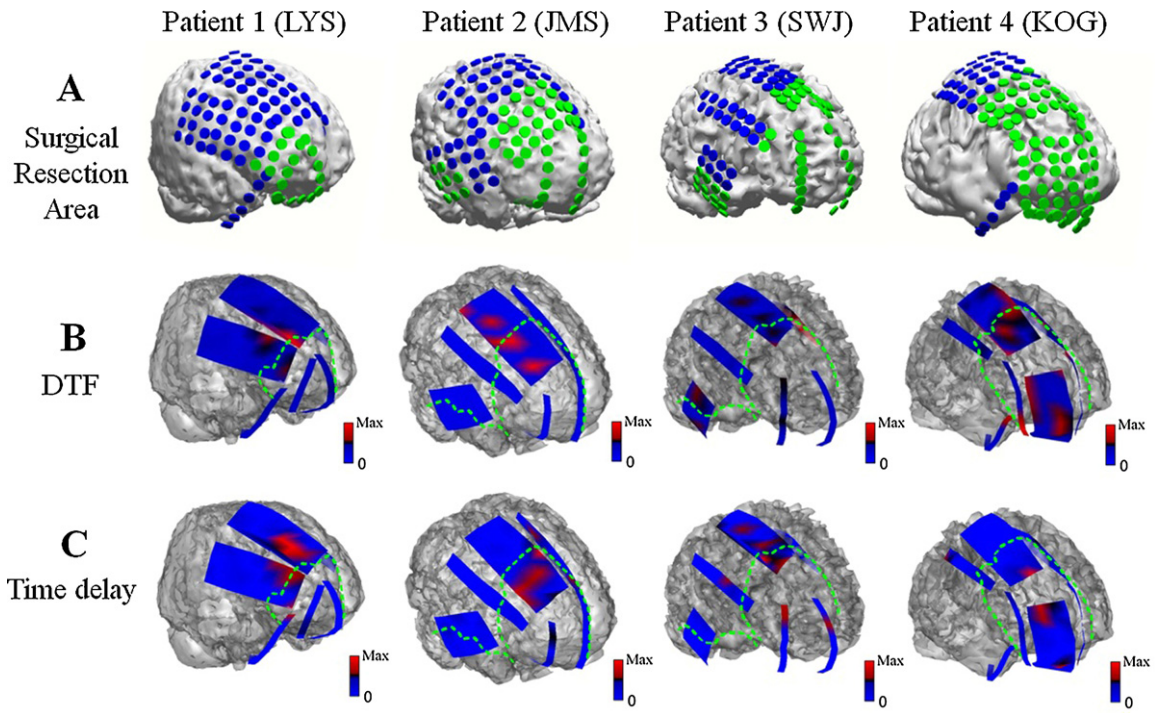

Figure 3 (a) Locations of subdural grid and strip electrodes and surgical resection areas of LGS patients (marked in green). (b) The distributions of average outflow values evaluated using the DTF analysis. Areas in red are regarded as potential ictal onset zones. (c) The distributions of average time delay values evaluated using information theoretical time delay analysis. Areas in red are regarded as potential ictal onset zones. Since electrodes with negative time delay values represent propagated activations, only the average time delay values exceeding zero (0) were visualized. (For interpretation of the references to color in this figure legend, the reader is referred to the web version of the article.)

and the average time delay distributions (Fig. 3c, third row) of four LGS patients. In most cases, the average outflow distributions and the average time delay distributions corresponded with each other. Moreover, the areas with high average time delay values coincided well with the surgical resection areas.

In the case of patient 1 (LYS), who underwent two epilepsy surgeries, first in the right frontal lobe and, 3 years later, in the posterior margin of the pre-resection site, both distributions acquired from the DTF analysis and the time delay analysis commonly showed high values around the right dorsolateral prefrontal cortex (DLPFC); these areas coincided well with the areas of surgical resection. As compared to the results of the DTF analysis, the time delay analysis resulted in rather widespread distributions located relatively posterior to the area of surgical resection.

On the contrary, in the case of patient 2 (JMS), who underwent surgical resection in the right frontal lobe and right inferior temporal lobe, the results of the time delay analysis coincided much better with the surgical resection areas than those of the DTF analysis. In the conventional DTF outflow distribution map, wide spurious signal generators appeared around the premotor cortex; whereas all the areas with high average time delay values were included in the area of surgical resection in the present time delay distribution map. Interestingly, in both computational iEEG analysis results, the middle and inferior temporal gyri included in the surgical resection areas were not identified as primary ictal onset zones. These results suggest that the epileptiform activity around the temporal lobe may be propagated from another region, although we were unable to test this hypothesis.

In the case of patient 3 (SWJ), who underwent two epilepsy surgeries, first in the right frontal lobe and then in the right inferior frontal gyrus and right inferior temporal lobe, both the DTF and time delay analysis results showed a few spurious distributions outside the surgical resection areas, e.g., superior temporal lobe and premotor cortex in the DTF results and premotor cortex in the time delay results. In the DTF analysis results, the strongest outflow values appeared around the superior frontal medial wall, whereas more widespread activities were included in the surgical resection areas in the time delay analysis results.

In patient 4 (KOG), who underwent a right frontal lobectomy, the ictal onset zones identified by the time delay analysis clearly better coincided with the surgical resection areas than those identified by the DTF analysis. The results of the DTF analysis were more widely distributed in the frontal lobe than those of the time delay analysis and included some unwanted spurious distributions in the superior parietal lobule. In both cases, the general patterns overlapped fairly well with the areas of surgical resection.

Discussion

LGS is one of the most intractable catastrophic epilepsies in children, characterized by multiple types of generalized

seizures, interictal bilaterally synchronous slow spike-waves and paroxysmal fast activity in EEGs, as well as progressive cognitive impairment (Heiskala, 1997). Most patients with LGS have bilateral diffuse encephalopathy, but focal lesions that contribute to secondary generalized epileptic encephalopathy can be identified using other localized EEG findings, such as persistent localized polymorphic slowings, spindle-shaped fast activities, localized paroxysmal fast activities, focal subclinical seizure activities, brief ictal rhythmic discharges, and electrodecrements (Lee et al., 2010a). In addition, recent advances in neuroimaging techniques with MRI as well as PET/SPECT could improve the detection of partial lesions (Kim et al., 2009). Nevertheless, despite these conventional modalities, it is still difficult to correctly localize ictal onset zones in patients with LGS with abundant ictal/interictal generalized epileptiform discharges. There is great demand for additional refinement techniques to confirm ictal onset zones.

In the early 1980s, Gotman (1983) first introduced a method to estimate time delay between two EEG channels by evaluating coherence and phase spectra over a certain frequency range and applied the method to EEG signals acquired from both animals and patients with generalized epilepsy. He investigated the time delay between seizure discharges observed in the same area of different hemispheres in patients with generalized epilepsy but did not apply his method to the identification of ictal onset zones. Mars et al. (1985) applied their time delay estimation method to the delineation of epileptogenesis in patients with focal or generalized epilepsy. In their study, time delay analysis was used to identify the ictal onset zones in focal epilepsy but was not applied to the identification of ictal onset zones in generalized epilepsy. In animal model studies, Medvedev et al. (1996) measured time delay between two intracerebral EEG signals recorded from rats with primary generalized epilepsy, from which they showed that the signal from the frontal cortex preceded that from the other area. Meeren et al. (2002) estimated time delay in rats with absence epilepsy and demonstrated the existence of a cortical focus that derived widespread corticothalamic networks during spontaneous absence seizures in the frontal lobe. To the best of our knowledge, our study is the first to apply time delay analysis to the localization of ictal onset zones in any type of human generalized epilepsy.

Among the various approaches to estimating time delay between two time series, we adopted the information theoretical time delay analysis method because the use of mutual information had some advantages over the other methods based on fast Fourier transform (FFT) in the analysis of LGS patient iEEG data, in that the FFT-based methods intrinsically require large data samples and stationary inputs (Harris et al., 1994; Jiruška et al., 2005). Contrary to the frequency-domain analysis methods, the information theoretical time delay estimation methods do not require any transformation of time series to the frequency domain and thus can analyze short signals with better accuracy (Moddemeijer, 1988). Moreover, the use of mutual information could provide more robust time delay estimates among signals with non-stationary or nonlinear characteristics. Indeed, Mars et al. (Mars and van Arragon, 1982; Mars and Lopes Da Silva, 1983; Mars et al., 1985) and Moddemeijer (1988) developed a time delay analysis method based on mutual information and demonstrated robust estimation of time delays among non-stationary signals. Considering that the ictal iEEG waveforms acquired from our LGS patients showed relatively short ictal duration time (<2 s in most ictal events) as well as non-stationary trends around the ictal onset time, the use of the mutual information-based time delay estimation method was more appropriate.

The present study demonstrated that ictal onset zones in pediatric patients with LGS could be precisely identified by applying the information theoretical time delay analysis to ictal iEEG recordings despite the generalized characteristics of ictal epileptiform activities. To the best of our knowledge, this paper introduced the first case studies reporting the possibility of using time delay analysis for the localization of ictal onset zones in patients with secondary generalized epilepsy. For each subject included in our analysis, the cortical areas with high average time delay values coincided well with the surgical resection areas determined by epileptologists based on multimodal neuroimaging results. Our results suggest that time delay analysis can be used as a promising auxiliary tool to confirm the ictal onset zones identified using other neuroimaging modalities. Furthermore, the ictal onset zones identified by the time delay analysis showed similar distributions to those identified by DTF analysis but showed slightly better coincidence with the surgical resection areas than those from the DTF analysis, suggesting that the complementary use of the DTF analysis and time delay analysis would enhance the overall accuracy of the localization of ictal onset zones in LGS.

Since the present time delay analysis basically assumes that the ictal onset zones are included in the recording sites, incorrect placement of iEEG electrodes may not guarantee the successful localization of ictal onset zones. Therefore, in addition to the current time delay analyses applied only to four successfully operated LGS patients, whose electrode placements proved to be correct, it would be an interesting future research topic to apply the same approach to more numbers of subjects including patients whose electrode placements were not correct. Moreover, since we applied our analysis method only to patients who became seizure free postoperatively, our next research topic should be the application of the present analysis method to other patients who did not become seizure free and the comparison of the localized ictal onset zones with their surgical resection areas, from which we hope to investigate whether the ictal onset zones localized by our approach were not completely removed in the surgery. We are currently planning to apply the time delay analysis to the other LGS patients' data, which were not considered in this study, with the aim to investigate whether the present time delay analysis can also be used to predict surgical outcomes before surgery or estimate correctness of iEEG electrode placement.

Although our study presented only four case studies, it is noteworthy that the time delay analysis provided more focalized ictal onset zones than the actual surgical resection areas in all cases, demonstrating the possibility of reducing the area for surgical resection. Particularly in the cases of subject 2 (JMS) and subject 3 (SWJ), the surgical resection area in the inferior temporal lobe was not identified by time delay analysis or by the conventional DTF analysis. Considering that the conventional neuroimaging modalities provided rather crude estimates of ictal onset zones

in secondary generalized epilepsy, as is easily observed in Table 1, it is expected that the localization of ictal onset zones using ictal iEEG would not only serve as an auxiliary imaging modality for pre-surgical evaluation, but also provide another opportunity to investigate the epileptogenesis of secondary generalized epilepsy. In future studies, more extensive computational iEEG analyses using massive clinical epilepsy iEEG data will be performed to quantitatively compare the performances of various neuroimaging modalities used for the delineation of epileptogenic zones in secondary generalized epilepsy. In addition to the present time delay estimation methods, some new computational iEEG analysis methods have been recently introduced to localize ictal and interictal epileptogenic zones, such as stochastic qualifiers (Prusseit and Lehnertz, 2007), adaptive DTF (Wilke et al., 2009), and high frequency analysis (Worrell et al., 2004). Therefore, one of the promising topics we hope to explore in future studies is the quantitative comparison of performances among various iEEG analysis methods for the localization of ictal onset zones, with the aim of demonstrating the usefulness of each iEEG analysis method and determining the most reliable method.

Acknowledgments

This work was supported in part by the KRISS-WCL project (Development of Measurement Technology for Cognitive Process) and in part by the research fund of Hanyang University (HY-2011-N).

References

Behrens, E., Zentner, J., Van Roost, D., Hufnagel, A., Elger, C.E., Schramm, J., 1994. Subdural and depth electrodes in the presurgical evaluation of epilepsy. Acta. Neurochir. 128, 84—87.

Binnie, C.D., Elwes, R.D.C., Polkey, C.E., Volans, A., 1994. Utility of stereoelectroencephalography in preoperative assessment of temporal lobe epilepsy. J. Neurol. Neurosurg. Psychiatry 57, 58—65.

Brazier, M.A.B., 1972. Spread of seizure discharges in epilepsy: anatomical and electrophysiological considerations. Exp. Neurol. 36, 263—272.

Cover, T.M., Thomas, J.A., Wiley, J., 1991. Elements of Information Theory. Wiley, New York.

Ding, L., Worrell, G.A., Lagerlund, T.D., He, B., 2007. Ictal source analysis: localization and imaging of causal interactions in humans. NeuroImage 34, 575—586.

Dubeau, F., McLachlan, R.S., 2000. Invasive electrographic recording techniques in temporal lobe epilepsy. Can. J. Neurol. Sci. 27, S29—S34.

Eichler, M., 2006. On the evaluation of information flow in multivariate systems by the directed transfer function. Biol. Cybern. 94, 469—482.

Gotman, J., 1983. Measurement of small time differences between EEG channels: Method and application to epileptic seizure propagation. Electroencephalogr. Clin. Neurophysiol. 56, 501—514.

Gotman, J., 1981. Interhemispheric relations during bilateral spike-and-wave activity. Epilepsia 22, 453—466.

Harris, B., Gath, I., Rondouin, G., Feuerstein, C., 1994. On time delay estimation of epileptic EEG. IEEE Trans. Biomed. Eng. 41, 820—829.

Heiskala, H., 1997. Community-based study of Lennox—Gastaut syndrome. Epilepsia 38, 526—531.

Jiruška, P., Prokš, J., Drbal, O., Sovka, P., Marusič, P., Mareš, P., 2005. Comparison of different methods of time shift measurement in EEG. Physiol. Res. 54, 459—465.

Jung, Y.J., Kang, H.C., Choi, K.O., Lee, J.S., Kim, D.S., Cho, J.H., Kim, S.H., Im, C.H., Kim, H.D., 2011. Localization of ictal onset zones in Lennox—Gastaut syndrome using directional connectivity analysis of intracranial electroencephalography. Seizure 20, 449—457.

Kaminski, M.J., Blinowska, K.J., 1991. A new method of the description of the information flow in the brain structures. Biol. Cybern. 65, 203—210.

Kim, J.T., Bai, S.J., Choi, K.O., Lee, Y.J., Park, H.J., Kim, D.S., Kim, H.D., Lee, J.S., 2009. Comparison of various imaging modalities in localization of epileptogenic lesion using epilepsy surgery outcome in pediatric patients. Seizure 18, 504—510.

Kobayashi, K., Ohtsuka, Y., Oka, E., Ohtahara, S., 1992. Primary and secondary bilateral synchrony in epilepsy: differentiation by estimation of interhemispheric small time differences during short spike-wave activity. Electroencephalogr. Clin. Neurophysiol. 83, 93—103.

Lee, Y.J., Kang, H.C., Lee, J.S., Kim, S.H., Kim, D.S., Shim, K.W., Lee, Y.H., Kim, T.S., Kim, H.D., 2010a. Resective pediatric epilepsy surgery in Lennox—Gastaut syndrome. Pediatrics 125, 58—66.

Lee, Y.J., Kang, H.C., Bae, S.J., Kim, H.D., Kim, J.T., Lee, B.I., Heo, K., Jang, J.W., Kim, D.S., Kim, T.S., Lee, J.S., 2010b. Comparison of temporal lobectomies of children and adults with intractable temporal lobe epilepsy. Childs. Nerv. Syst. 26, 177—183.

Marple, L.S., Nuttall, A.H., 1983. Experimental comparison of three multichannel linear prediction spectral estimators. In: IEE Proceedings, Part F: Communications, Radar and Signal Processing, vol. 130, pp. 218—229.

Mars, N.J.I., Lopes da Silva, F.H., 1987. EEG analysis methods based on information theory. In: Gevins, A.S., Remond, A. (Eds.), Methods of Analysis of Brain Electrical and Magnetic Signals: EEG Handbook. Elsevier, Amsterdam, pp. 279—307.

Mars, N.J.I., Thompson, P.M., Wilkus, R.J., 1985. Spread of epileptic seizure activity in humans. Epilepsia 26, 85—94.

Mars, N.J.I., Lopes Da Silva, F.H., 1983. Propagation of seizure activity in kindled dogs. Electroencephalogr. Clin. Neurophysiol. 56, 194—209.

Mars, N.J.I., van Arragon, G.W., 1982. Time delay estimation in non-linear systems using average amount of mutual information analysis. Signal Process. 4, 139—153.

Medvedev, A., Mackenzie, L., Hiscock, J.J., Willoughby, J.O., 1996. Frontal cortex leads other brain structures in generalised spike-and-wave spindles and seizure spikes induced by picrotoxin. Electroencephalogr. Clin. Neurophysiol. 98, 157—166.

Meeren, H.K.M., Pijn, J.P.M., Van Luijtelaar, E.L.J.M., Coenen, A.M.L., Da Silva, F.H.L., 2002. Cortical focus drives widespread corticothalamic networks during spontaneous absence seizures in rats. J. Neurosci. 22, 1480—1495.

Moddemeijer, R., 1988. An information theoretical delay estimator. In: Ninth Symposium on Information Theory in the Benelux, Enschede (NL), vol. 12, pp. 1—128.

Neumaier, A., Schneider, T., 2001. Estimation of parameters and eigenmodes of multivariate autoregressive models. CM Trans. Math. Softw. 27, 27—57.

Palmini, A., Najm, I., Avanzini, G., Babb, T., Guerrini, R., Foldvary-Schaefer, N., Jackson, G., Lüders, H.O., Prayson, R., Spreafico, R., Vinters, H.V., 2004. Terminology and classification of the cortical dysplasias. Neurology 62, S2—S8.

Pondal-Sordo, M., Diosy, D., Téllez-Zenteno, J.F., Sahjpaul, R., Wiebe, S., 2007. Usefulness of intracranial EEG in the decision process for epilepsy surgery. Epilepsy Res. 74, 176—182.

Prusseit, J., Lehnertz, K., 2007. Stochastic qualifiers of epileptic brain dynamics. Phys. Rev. Lett. 98, 1—4.

Rosenow, F., Lüders, H., 2001. Presurgical evaluation of epilepsy. Brain 124, 1683—1700.

Schlögl, A., 2006. A comparison of multivariate autoregressive estimators. Signal Process. 86, 2426—2429.

Schreiber, T., 2000. Measuring information transfer. Phys. Rev. Lett. 85, 461—464.

Schreiber, T., Schmitz, A., 1996. Improved surrogate data for nonlinearity tests. Phys. Rev. Lett. 77, 635—638.

Schwarz, G., 1978. Estimating the dimension of a model. Ann. Statistics 6, 461—464.

Strand, O.N., 1977. Multichannel complex maximum entropy (autoregressive) spectral analysis. IEEE Trans. Automat. Control. 22, 634—640.

Swiderski, B., Osowski, S., Cichocki, A., Rysz, A., 2009. Single-class SVM and directed transfer function approach to the localization of the region containing epileptic focus. Neurocomputing 72, 1575—1583.

Talantzis, F., Constantinides, A.G., Polymenakos, L.C., 2005. Estimation of direction of arrival using information theory. IEEE Signal Process. Lett. 12, 561—564.

Theiler, J., Eubank, S., Longtin, A., Galdrikian, B., Doyne Farmer, J., 1992. Testing for nonlinearity in time series: the method of surrogate data. Physica D 58, 77—94.

Wilke, C., van Drongelen, W., Kohrman, M., He, B., 2010. Neocortical seizure foci localization by means of a directed transfer function method. Epilepsia 51, 564—572.

Wilke, C., van Drongelen, W., Kohrman, M., He, B., 2009. Identification of epileptogenic foci from causal analysis of ECoG interictal spike activity. Clin. Neurophysiol. 120, 1449—1456.

Wilson, S.B., Emerson, R., 2002. Spike detection: a review and comparison of algorithms. Clin. Neurophysiol. 113, 1873—1881.

Worrell, G.A., Parish, L., Cranstoun, S.D., Jonas, R., Baltuch, G., Litt, B., 2004. High-frequency oscillations and seizure generation in neocortical epilepsy. Brain 127, 1496—1500.

Wyllie, E., Lachhwani, D.K., Gupta, A., Chirla, A., Cosmo, G., Worley, S., Kotagal, P., Ruggieri, P., Bingaman, W.E., 2007. Successful surgery for epilepsy due to early brain lesions despite generalized EEG findings. Neurology 69, 389—397.